

# Analysis of the electrophoretic profiles of prion protein in carcinous and pericarcinous lysates of six different types of cancers

**Wei Wei**

Beijing Cancer Hospital

**Qi Shi**

Centers for Disease Control and Prevention

**Yue-Zhang Wu**

Centers for Disease Control and Prevention

**Xue-Hua Yang**

Centers for Disease Control and Prevention

**Kang Xiao**

Centers for Disease Control and Prevention

**Xiaoping Dong** (✉ [dongxp238@sina.com](mailto:dongxp238@sina.com))

China CDC

---

## Research article

**Keywords:** Prion protein, cancers, electrophoretic profiles

**Posted Date:** March 16th, 2020

**DOI:** <https://doi.org/10.21203/rs.3.rs-17368/v1>

**License:** © ⓘ This work is licensed under a Creative Commons Attribution 4.0 International License.

[Read Full License](#)

---

# Abstract

**Introduction** PrP (Prion Protein) is a cellular membrane protein distributing in many kinds of tissue cells. Besides its critical role in prion disease, the potential roles of cellular PrP in human malignant tumors have been also addressed. However, the profiles of PrP in malignant tumors, such as the patterns in electrophoresis and biochemistry features, are still not well known.

**Objective** To find the different electrophoretic profiles of prion protein in carcinous and pericarcinous lysates of six different types of cancers.

**Methods** Western Blot was used to test the amounts of total PrP in cancer samples and the tolerance of PK (protease K) digestion among various tissue types.

**Results** A mass of the PrP signals with large molecular weight were identified in the homogenates of peripheral tissues. The amounts of total PrP evaluated by Western blots did not differ significantly between carcinous and pericarcinous tissues. PrPs in all types of the tested cancer samples were PK sensitive, but showed diversity in the tolerance of PK digestion among various tissue types.

**Conclusions** The electrophoretic patterns of carcinous and pericarcinous tissues were almost similar, but markedly different from that of brain tissues.

## Background

PrP is a cellular membrane protein distributing in many kinds of tissue cells. PrP become attractive due to its conformational changed isoform PrP<sup>Sc</sup>, which is the etiological agent for prion disease or transmissible spongiform encephalopathy (TSE). In this theory, the normal and physiological form of PrP (PrP<sup>C</sup>) converts to abnormal and pathological isoform, leading to a pathogenesis of special neurodegenerative disease with markedly short clinical course and 100% fatal rate[1]. As a conservative cellular protein, the have been proposed, such as cell signal transduction, cellular copper metabolism, cell adhesion, anti-apoptosis, migration, immune modulation and cell differentiation[2]. However, depletion of PrP expression in the knock out transgenic mouse does not affect the development and function of central nerve system and even life span[3].

PrP is a glycosylating protein, with two N-linked glycosylating sites at codon 181 Ser and 197 Ser at its C-terminus. According to the glycosylation on those sites, three main forms of PrP molecules can be seen, di-, mono- and aglycosylated PrPs, with about 5 kDa difference each glycosylation site[4]. In brain tissues, three normal PrP<sup>C</sup> bands migrate from 25 to 35 kDa in SDS-PAGE. In the brains of prion diseases, e.g., human sporadic Creutzfeldt-Jacob disease (sCJD) and scrapie infected experimental rodent, amounts of large molecular weight PrP signals are usually observable in the Western blots, besides of accumulation of lager amount of three forms of PrP monomers[5]. More importantly, the pathological PrP<sup>Sc</sup> possesses partially proteinase K (PK) resistance, proteolyzing the N-terminal fragment and leading to produce three

truncated PrP bands ranging from 19 to 25 kDa when exposed to PK digestion. Such characteristics are used to distinguish PrP<sup>C</sup> and PrP<sup>Sc</sup> in brain tissues of prion disease[6].

Besides of its critical role in prion disease, the potential roles of cellular PrP in human malignant tumors have been also addressed. Using immunohistochemical techniques, overexpression of PrP has been identified in a variety of malignant tumors, including laryngeal, gastric, pancreatic and breast carcinomas, osteosarcoma and melanoma [7]. Overexpression of PrP is proposed to be closely associated with poor prognosis of pancreatic and breast cancers, highlighting that PrP may affect the growth and invasiveness of cancers. Study also has demonstrated an important role of overexpression of PrP in the acquisition of multi-drug resistant gastric cancer[8]. However, the profiles of PrP in malignant tumors, such as the patterns in electrophoresis and biochemistry features, are addressed little.

To see the profiles of PrP molecules in malignant tumors, we collected different numbers of the surgically removed samples of gastric, colon, liver, lung, thyroid and laryngeal cancers, as well as the individual pericarcinous tissues. After preparation of tissue homogenates, PrP specific Western blots were conducted. We found that the electrophoretic patterns of carcinous and pericarcinous tissues were similar, but markedly different from that of brain tissues. The amounts of total PrP evaluated by Western blots did not differ significantly between carcinous and pericarcinous tissues. PrPs in all types of the tested cancers were PK sensitive, but showed diversity in the tolerance of PK digestion among various tissue types.

## Methods

### Specimens

All cancer specimens were collected from Peking University Cancer Hospital & Institute with pathological diagnosis. The cancer and pericarcinous tissues were removed surgically and frozen at -80 °C for further usage. The specimens tested in this study included 10 gastric cancers, 5 colon cancers, 5 liver cancers, 9 lung cancers, 10 thyroid cancers and 10 laryngeal cancers.

### Preparations of tissue homogenates

Tissue samples from various carcinomas and the pericarcinous tissues, as well as from human and hamster brains were washed in Tris-buffered saline (TBS, 10 mM Tris-HCl, 133 mM NaCl, pH7.4) for at least three times. Each sample was mixed in the lysis buffer (100 mM NaCl, 10 mM EDTA, 0.5% NP-40, 0.5% sodium deoxycholate, 10 mM Tris, pH 7.4) containing protease inhibitor cocktail set III at the ratio of 1:10 (w/v) and then homogenized mechanically. The preparations were centrifuged at 2000 × g for 10 min or 20000 × g for 30 min to discard the tissue debris and the supernatant fractions were collected separately and stored at -80 °C for further experiments.

### Western blots

Aliquots of tissue homogenates were separated in 12% SDS-PAGE and electroblotted onto nylon membranes with semi-dry facility. Membranes were blocked in TBS containing 5% skimmed milk at room temperature (RT) for 2 h and incubated with various primary antibodies at 4 °C overnight, including PrP specific monoclonal antibodies (mAb) 3F4, 4H2, 6D11, 7D9, 8H4 and SAF32, and anti- $\beta$ -actin antibody (1:5,000, huaxingbio, HX1827). After washing with TBS containing 0.1% Tween 20 (TBST), the membranes were incubated with HRP conjugated secondary antibodies (Jackson ImmunoResearch Labs, 115-035-003 and 111-035-003) at RT for 1 h. The blots were developed using enhanced chemiluminescence system (ECL, PerkinElmer, NEL103E001EA) and visualized on autoradiography films (General Electrics).

## **Proteinase K (PK) digestion**

To evaluate the PK-resistances of PrP proteins in cancer tissues, 10% tissue homogenates were exposed to different concentrations of PK, including 20, 50, 100, 250, 500 and 1000  $\mu$ g/ml. The digestion was performed at 37 °C for 1 h and stopped by boiling in loading buffer. The preparations were immediately subjected in to SDS-PAGE and Western blots with mAb 3F4. For positive control of PrP<sup>Sc</sup>, 10% brain homogenates of human sCJD or 263K-infected hamster was incubated with a final concentration of 20  $\mu$ g/ml proteinase K at 37 °C for 1 h prior to Western blots.

## **PrP deglycosylation**

15  $\mu$ l-aliquot of tissue homogenates were boiled for 10 minutes in denaturing buffer (0.5% SDS, 1%  $\beta$ -mercaptoethanol), and deglycosylated with 1500 U PNGase F (Biolab) in 1% Nonidet P-40, 50 mM sodium phosphate, pH 7.5 at 37 °C for 12 hr. Proteins were precipitated with 4 volumes of cold methanol at -20°C for 6 hr and centrifuged at 15,000 g for 30 minutes. The pellets were resuspended and separated in 12% SDS-PAGE and PrP specific Western blots with mAb 3F4.

## **Statistical assays**

The blot images of Western blots were captured by ChemiDoc™ XRS + Imager and quantified by Image J software. Statistical analyses were performed using Student's t test. All data were presented as the mean + SEM.

## **Results**

### **The PrPs in the tissues of the malignant tumors show different electrophoretic patterns in Western blots compared with that of brain tissues**

To see the presence and the electrophoretic profiles of the PrP proteins in the malignant tissues, three randomly selected prepared tissue homogenates of each type of cancers were pooled and subjected into Western blots with PrP mAb 3F4. In parallel, the brain homogenates from a sCJD case and a normal donator died of car accident, as well as that of scrapie agent 263K-infected hamster were loaded as the

control. Clear three PrP specific bands were observed in the preparations of brain specimens, which were at the positions from 25 to 35 kDa representing di-, mono- and non-glycosylated PrPs (Fig 1). Additionally, larger molecular weights of PrP-specific signals were also detected in the brain homogenates of sCJD and 263-infected hamster. In contrast, the pooled samples of cancer tissues displayed the distinguishing electrophoretic patterns, containing more positive blotted bands (Fig 1). The most predominate bands were larger molecular weight signals, which migrated at almost the same position as those in the brain homogenates. There was relatively weak but clear positive band at the position of monoglycosylated PrP in all tumor preparations, and the bands at the position of aglycosylated PrP in some preparations, but no clear band corresponding to diglycosylated PrP (Fig 1). Additionally, the PrP reactive patterns in Western blot of all tested cancers seemed to be similar and the amounts of PrP positive signals were also undistinguished after digital assays of the gray values of all PrP signals (Fig 1).

To further assess the glycosylating features of PrP signals in tumor tissues, the homogenates of three laryngeal carcinomas and two benign polyps were undergone into the process of deglycosylation together with or without PK digestion. In the reaction of PNGase F without PK treatment (Fig 2A, middle panel), all tested laryngeal samples revealed distinct PrP signals at the position of 25 kDa approximately, which migrated at the same position as the brain samples of healthy or diseased human and hamster. Besides, a weak and small molecular signal was also observed in some malignant tissues, which looked to be slightly higher in SDS-PAGE than those of brain tissues. In the preparation of PNGase F after 20 µg/ml PK-digestion (Fig 2A, bottom panel), as expected, the PrP signals in the normal human and hamster brain samples disappeared and those in sCJD case and 263K-infected hamster shifted to the position slightly higher of 20 kDa. PrP specific signals were still detectable in the three tested malignant cancers that seemed to be still slightly higher than those in TSE brain samples. No or very faint PK-resistant PrP signal was observed in the homogenates of two benign laryngeal polyps.

Subsequently, the immunoreactivities of PrP signals in tumor tissues were tested by Western blots with various PrP specific antibodies. The recognizing peptides within PrP of those antibodies were illustrated in Fig 2B (upper panel). The pooled samples from three gastric cancers and the pooled samples of the pericarcinous tissues from the same three cases were subjected into the tests, using the brains of 263K-infected hamster as the control. As shown in Fig 2B, two predominate PrP bands were observed in all reactions, one was large molecular weight signal and the other was at the position of monoglycosylated PrP. In addition to the difference in signal strength, the reactive profiles to various PrP antibodies looked to be similar. Meanwhile, PrP reactive profiles in carcinous and pericarcinous tissues were also quite comparable. It indicates that the PrPs in the cancer tissues are probably full-length ones.

**There is no significant difference in PrP amount evaluated by Western blots between carcinous and pericarcinous tissues**

The changes of PrP in various kinds of human malignant tissues are widely described, among them most are based on immunohistochemical assays[9]. To evaluate the potential difference in PrP amount in Western blots between the carcinous and pericarcinous tissues, different numbers of gastric, colon, liver, lung, thyroid and laryngeal cancers were employed into Western blots with mAb 3F4, together with the individual pericarcinous tissues in parallel. In general, the PrP reactive patterns were similar between carcinous and pericarcinous tissues (Fig 3). The signal intensity among the different cases in some special types of cancers varied. Quantitative assays of the average gray values of total PrP signals after normalized with the individual actin showed slightly higher in the carcinous tissues of gastric (Fig 3A), liver (C), thyroid (E) and laryngeal (F) cancers, while slightly higher in the pericarcinous tissues of colon (B) and lung (D), but without statistical significance. It highlights that under our experimental condition, either PrP reactive profiles or intensities in the carcinous and pericarcinous tissues are undistinguishable by the Western blots.

## **The PrPs in the carcinous and pericarcinous tissues are PK-sensitive, but vary among the tissue types**

To test the features of PK-resistance of PrPs in various tumors, the pooled carcinous and pericarcinous samples consisting of randomly selected three cases were prepared. After exposed to different concentrated PK for 1 hr, the digestions were stopped and subjected into Western blots immediately. As shown in Fig 4, the PrP signals in all tested tissue kinds of carcinous and pericarcinous samples were reduced in dose-dependent manner. PrPs in all types of the tissues were partially but clearly PK resistant to the digestion of 20 µg/ml. At the same PK working concentration (20 µg/ml), the PrP signal in the normal brain homogenates vanished completely (data not shown). Along with the increase of PK amount, the PrP signals of large molecular weight completely disappeared, whereas those of small molecular weight were remarkably weaker and eventually undetectable. Different tissue types seemed to show slight diversity of PK-resistances. Quantitative measures of the average gray values revealed that PrP signals in gastric (Fig 4 A) and colon (D) tissues reduced to 20-60% in the reaction of 20 µg/ml, and less than 7% in the reaction of 50 µg/ml compared with that without PK. The PrP signals in the tissues of liver (C), lung (D) and thyroid (E) seemed to be more sensitive to PK digestion, which reduced to almost undetectable in the preparation of 50 µg/ml PK. The PrP signals in laryngeal tissues (F) were markedly more PK-resistant, which maintained 70% signals in the reaction of 20 µg/ml and about 25% in that of 50 µg/ml PK. Comparison of the PK-resistance of PrP signals in carcinous and pericarcinous tissues proposed a tendency that the PrP signals in malignant tissues had slightly stronger tolerance to PK digestion. Those data indicate that the PrPs in the malignant tumors are generally PK sensitive, despite of slightly more tolerant to PK digestion than the PrPs in brains.

## **Discussion**

In this study, we have screened the electrophoretic and immunoreactive patterns of PrPs in a numbers of six types of human malignant tumors and their pericarcinous tissues. All tested samples, regardless of carcinous or pericarcinous tissues, contain the similar PrP electrophoretic patterns that are distinctively different from that of brain tissues, regardless normal or prion disease. Furthermore, we have also tested the PrP electrophoretic patterns in different tissue homogenates from normal mice, including heart, liver, spleen and lung. As indicated in Supp Fig. 3, similar PrP electrophoretic profiles are observed, showing predominate amounts of lager molecular weight PrP signals. We have even prepared the tissue homogenates with different centrifuging speeds (2,000 and 20,000 rpm) in order to exclude the possible influence of tissue debris in SDS-PAGE. There is little change in the PrP patterns, besides of slight increase of the amounts of PrP monomers in some tissues, e.g., heart and lung (Supp Fig. 1). It seems that the PrP electrophoretic patterns do not associate with the malignancy, but reflect the feather of PrP in the peripheral tissues.

We have found that there are large quantities of PrP signals with large molecular weight in the homogenates of peripheral tissues. Among them, the bands roughly at the position 55 kDa are predominating. Such large molecular weight PrP signals can be also observed in the homogenates of brain tissues, especially in the brains of prion diseases, but showing apparently less amounts compared with the PrP monomers[10]. Although we do not have the direct sequence data for such bands, based on the molecular weight and the immunoreactivity to PrP antibodies, such bands might be the dimer of PrP molecules. PrP dimer is observable in normal brain tissues, in some cultured mammalian cells and even in the prokaryotic lysates expressing recombinant PrP[11]. As the smallest aggregate, PrP dimer can be disulfide-bonded or non-disulfide linked [12]. Based on the recombinant human PrP proteins, they even illustrate that three motifs with PrP peptide modulate PrP dimerization, the negative motif of residues 36–42, and positive ones of residues 90–125 and residues 195–212[13]. Our data here indicates that the majority of PrP molecules in the lysates of peripheral tissues seem to be the full-length PrP, as the wide reactivities with various PrP mAbs of different recognizing sites and the generation of single PrP bands after treatment of PNGase F. More aggregative forms of PrP, represented by PrP dimers, in the peripheral tissues than in brain tissues may suggest diverse PrP post-translational modifications.

Our PrP specific Western blots do not figure out significant difference either in the pattern or in the amount of PrPs between the carcinous and pericarcinous tissues. Overexpression of PrP in a number of malignant tumors has been documented repeatedly, but most of the studies are conducted with PrP specific IHC assays [14–16]. The exact reason for such diversity using different techniques is known, although with the same PrP mAbs. One possibility is that the PrP antibodies recognize only linear epitope in Western blot, while react with both linear and conformational epitopes in IHC. The stronger PrP signals of carcinous slices in IHC tests might derive from the reactions of PrP conformational epitopes with PrP specific antibodies. Nevertheless, the overexpression of PrP in carcinous tissues by IHC is not observable by routine PrP-specific Western blots.

We have found that the PrPs in the peripheral tissues show weak PK-resistances that are slightly but obviously stronger than the PrPs in brain tissues. The PK-resistances of the PrPs from different tissue

lysates look also slightly different. PrPs in laryngeal tissues are more PK-resistant, followed by the PrP in stomach and colon, while PrPs from liver, lung and thyroid tissues are less. Normal PrP proteins show PK-resistance in the situation of aggregation. The PrP proteins with disease-associated mutations are more prone to form aggregates and to display PK-resistance in vitro[17]. Unlike the PrP<sup>Sc</sup> in prion diseases, those aggregated PrPs certainly do not have the infectivity[18]. More importantly, the PK-digested products of the aggregated normal and mutated PrPs usually do not shift down in the electrophoresis[19, 20], which means the conformational structures of the aggregated PrPs are different from that of PrP<sup>Sc</sup>. We may assume that the weak PK-resistances of PrPs in peripheral tissues are likely due to more PrP dimers and polymers.

## Conclusions

In summary, we observed the different electrophoretic profiles of prion protein in carcinous and pericarcinous lysates of six different types of cancers. Our finding are the amounts of total PrP evaluated by Western blots did not differ significantly between carcinous and pericarcinous tissues. PrPs in all types of the tested cancer samples were PK sensitive but showed diversity in the tolerance of PK digestion among various tissue types. So, the electrophoretic patterns of carcinous and pericarcinous tissues were almost similar, but markedly different from that of brain tissues.

## Abbreviations

PrP  
Prion Protein  
TSE  
Transmissible Spongiform Encephalopathy  
sCJD  
Sporadic Creutzfeldt-Jacob disease  
PK  
Protease K

## Declarations

### Ethics approval and consent to participate

This study is in accordance with the Declaration of Helsinki and has been approved by the Peking University Cancer Hospital & Institute. Written informed consent was obtained from the participants for sample collection and analysis.

### Consent for publish

Not applicable

### **Availability of data and materials**

All data generated or analyzed during this study are included in this published article and supplemental datas.

### **Competing interests**

The authors declare that they have no competing interests

### **Funding**

National Key R&D Program of China (2018ZX10711001), this work was supported by Chinese National Natural Science Foundation Grants (81630062) and Grant(2019SKLID501,2019SKLID603,2019SKLID307) from the State Key Laboratory for Infectious Disease Prevention and Control(China CDC).

### **Authors' Contributions**

WW collected the patients' samples and clinical data; WW and QS performed the research and wrote the first draft. YZ W performed the Western blot test; XHY and Kang Xiao performed the data Statistical analysis; XPD, who is the corresponding author, designed the study and revised the manuscript. All authors have read and approved the manuscript.

### **Acknowledgements**

Not applicable

### **Authors' Affiliations**

Key laboratory of Carcinogenesis and Translational Research (Ministry of Education), Head and Neck Surgery Department, Peking University Cancer Hospital & Institute, Beijing 100142, China.

Wei Wei

State Key Laboratory for Infectious Disease Prevention and Control, Collaborative Innovation Center for Diagnosis and Treatment of Infectious Diseases (Zhejiang University), National Institute for Viral Disease Control and Prevention, Chinese Center for Disease Control and Prevention, Chang-Bai Rd 155, Beijing 102206, China.

Qi Shi, Yue Zhang Wu, Xuehua Yang, Kang Xiao, Xiaoping Dong

Center for Global Public Health, Chinese Center for Disease Control and Prevention, Chang-Bai Rd 155, Beijing 102206, China

Xiaoping Dong

Wuhan Institute of Virology, Chinese Academy of Science, Xiao Hong Shan No.44, Wuhan, 430071, China.

Xiaoping Dong

China Academy of Chinese Medical Sciences, Dongzhimeinei, South Rd 16, Beijing 100700, China

Xiaoping Dong

## References

1. Asher, D.M. and L. Gregori, *Human transmissible spongiform encephalopathies: historic view*. *Handb Clin Neurol*, 2018. **153**: p. 1-17.
2. Watts, J.C., M.E.C. Bourkas, and H. Arshad, *The function of the cellular prion protein in health and disease*. *Acta Neuropathol*, 2018. **135**(2): p. 159-178.
3. Weissmann, C. and E. Flechsig, *PrP knock-out and PrP transgenic mice in prion research*. *Br Med Bull*, 2003. **66**: p. 43-60.
4. Fiorini, M., et al., *Biochemical Characterization of Prions*. *Prog Mol Biol Transl Sci*, 2017. **150**: p. 389-407.
5. Castle, A.R. and A.C. Gill, *Physiological Functions of the Cellular Prion Protein*. *Front Mol Biosci*, 2017. **4**: p. 19.
6. Lehmann, S., *[The prion protein]*. *J Soc Biol*, 2002. **196**(4): p. 309-12.
7. Yang, X., et al., *Prion protein and cancers*. *Acta Biochim Biophys Sin (Shanghai)*, 2014. **46**(6): p. 431-40.
8. Hinton, C., et al., *Significance of prion and prion-like proteins in cancer development, progression and multi-drug resistance*. *Curr Cancer Drug Targets*, 2013. **13**(8): p. 895-904.

9. Liang, J., et al., *Hypoxia induced overexpression of PrP(C) in gastric cancer cell lines*. *Cancer Biol Ther*, 2007. **6**(5): p. 769-74.
10. MacLea, K.S., *What Makes a Prion: Infectious Proteins From Animals to Yeast*. *Int Rev Cell Mol Biol*, 2017. **329**: p. 227-276.
11. Colby, D.W. and S.B. Prusiner, *Prions*. *Cold Spring Harb Perspect Biol*, 2011. **3**(1): p. a006833.
12. Taguchi, Y., et al., *Disulfide-crosslink scanning reveals prion-induced conformational changes and prion strain-specific structures of the pathological prion protein PrP(Sc)*. *J Biol Chem*, 2018. **293**(33): p. 12730-12740.
13. Gao, Z., et al., *Prion dimer is heterogenous and is modulated by multiple negative and positive motifs*. *Biochem Biophys Res Commun*, 2019. **509**(2): p. 570-576.
14. Wei, W., et al., *Expression of prion protein is closely associated with pathological and clinical progression and abnormalities of p53 in head and neck squamous cell carcinomas*. *Oncol Rep*, 2016. **35**(2): p. 817-24.
15. Zhou, L., et al., *Overexpression of PrPc, combined with MGr1-Ag/37LRP, is predictive of poor prognosis in gastric cancer*. *Int J Cancer*, 2014. **135**(10): p. 2329-37.
16. Diarra-Mehrpour, M., et al., *Prion protein prevents human breast carcinoma cell line from tumor necrosis factor alpha-induced cell death*. *Cancer Res*, 2004. **64**(2): p. 719-27.
17. Marrone, A., N. Re, and L. Storchi, *The Effects of Ca<sup>2+</sup> Concentration and E200K Mutation on the Aggregation Propensity of PrPC: A Computational Study*. *PLoS One*, 2016. **11**(12): p. e0168039.
18. Muramoto, T., *[Prion protein structure and its relationships with pathogenesis]*. *Rinsho Shinkeigaku*, 2003. **43**(11): p. 813-6.
19. Mishra, R., et al., *Impact of N-glycosylation site variants during human PrP aggregation and fibril nucleation*. *Biochim Biophys Acta Proteins Proteom*, 2019.
20. Paciotti, R., L. Storchi, and A. Marrone, *An insight of early PrP-E200K aggregation by combined molecular dynamics/fragment molecular orbital approaches*. *Proteins*, 2019. **87**(1): p. 51-61.

## Supplemental Figures

**Supplemental Figure 1.** Full-length blots of Figure1

**Supplemental Figure 2.** Full-length blots of Figure2

**Supplemental Figure 3.** Western blots of the PrPs in the tissue homogenates of brain, heart, liver, spleen and lung of normal hamsters. The centrifuge speeds (rpm) for preparing the tissue homogenates are indicated at the bottom of the graph.

## Figures

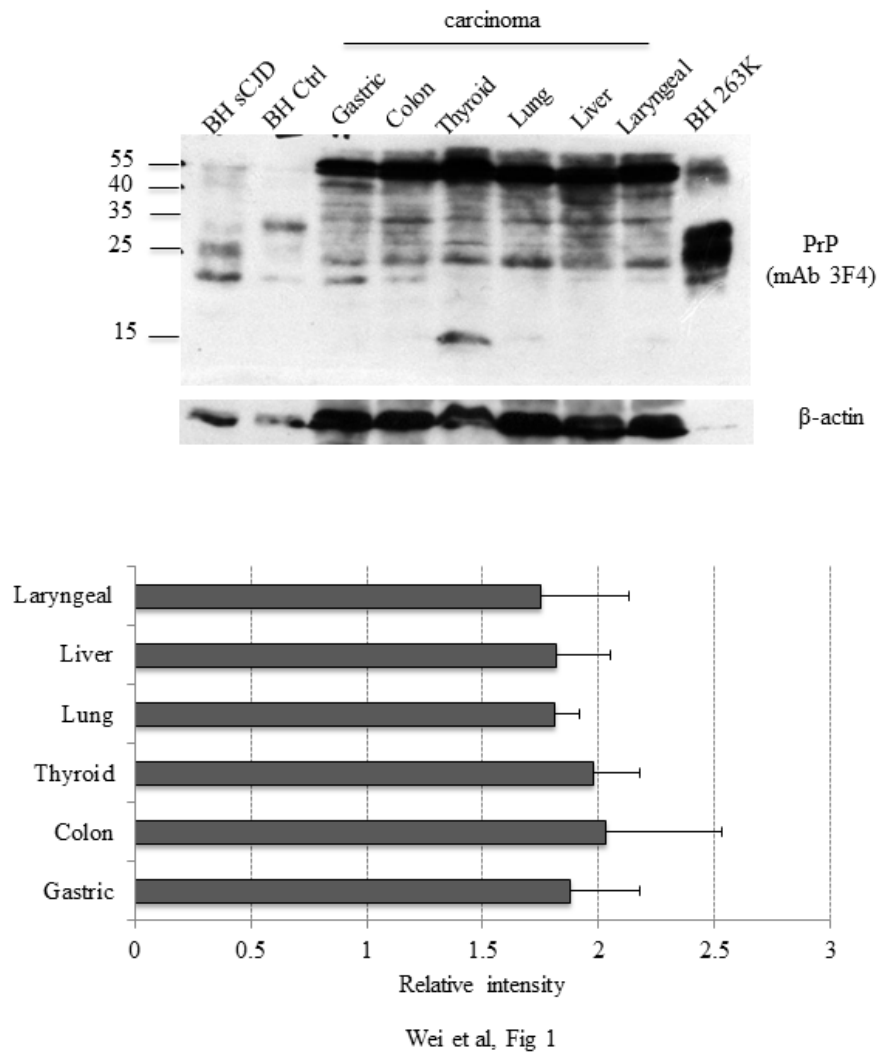


**Figure 1**

Representative PrP-specific Western blot of the pooled homogenates of six different cancer tissues (upper panel). Randomly selected the lysates of three individual carcinous tissues each cancer were mixed as the pooled homogenate. Brain homogenates (BH) of a normal person died of car accident, a sCJD patient and scrapie agent 263K-infected hamster were used as controls. All preparations were undergone into Western blot with PrP mAb 3F4 without PK digestion. The densities of signals are determined by densitometry of all PrP signals and showed as relative intensity after normalized with the individual values of  $\beta$ -actin. Graphical data denote mean+SD (bottom panel). Full-length blots were presented in Supplementary Figure1.

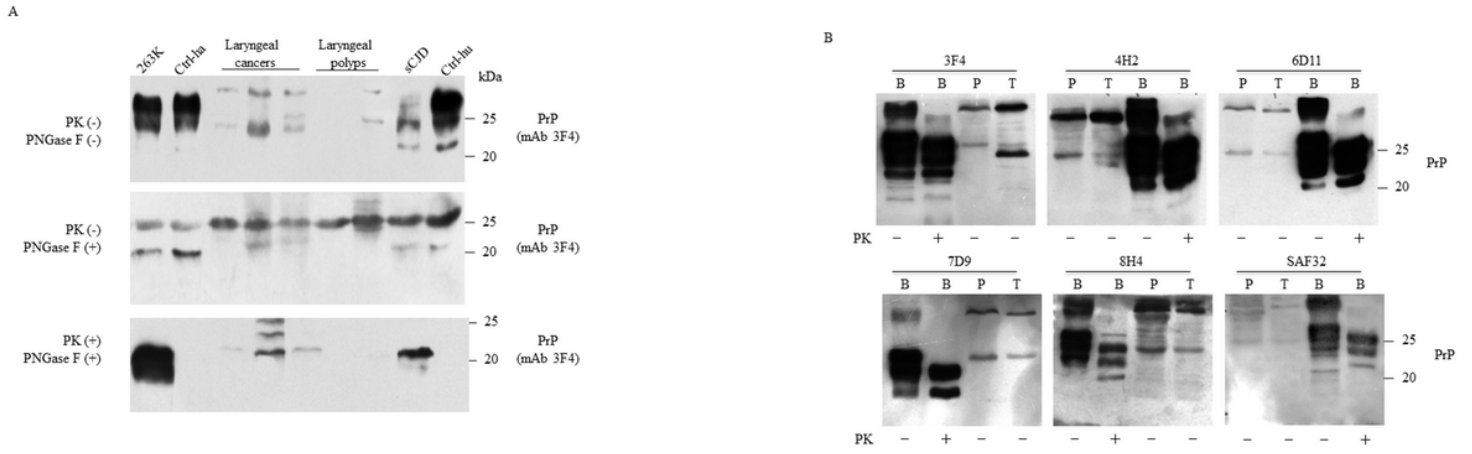


**Figure 2**

Evaluation of the glycosylating and immunoreactive features of PrPs in the carcinous tissues. A. Diglycosylation with PNGase F. The homogenates of three laryngeal carcinomas and two benign polyps were included, together with the brain lysates of normal and 263K-infected hamsters, as well as of normal donate and sCJD patients as controls. Upper panel: The lysates without treatment of PNGase and PK. Middle panel: The lysates treated with PNGase, but without PK. Lower panel: The lysates treated with PNGase and PK (20 µg/ml). B. Immunoreactivities with various PrP specific mAbs. The pooled homogenates of gastric carcinous and pericarcinous tissues were subjected into the Western blots with PrP specific mAbs 3F4, 4H3, 6D11, 7D9, 8H4 and SAF32, respectively. The brain lysates of 236K-infected hamster treated with PK (20 µg/ml) and without PK were loaded as controls. The loading volume for tumor homogenate is 20 µl and the volume for brain homogenate is 15 µl. Full-length blots were presented in Supplementary Figure2.

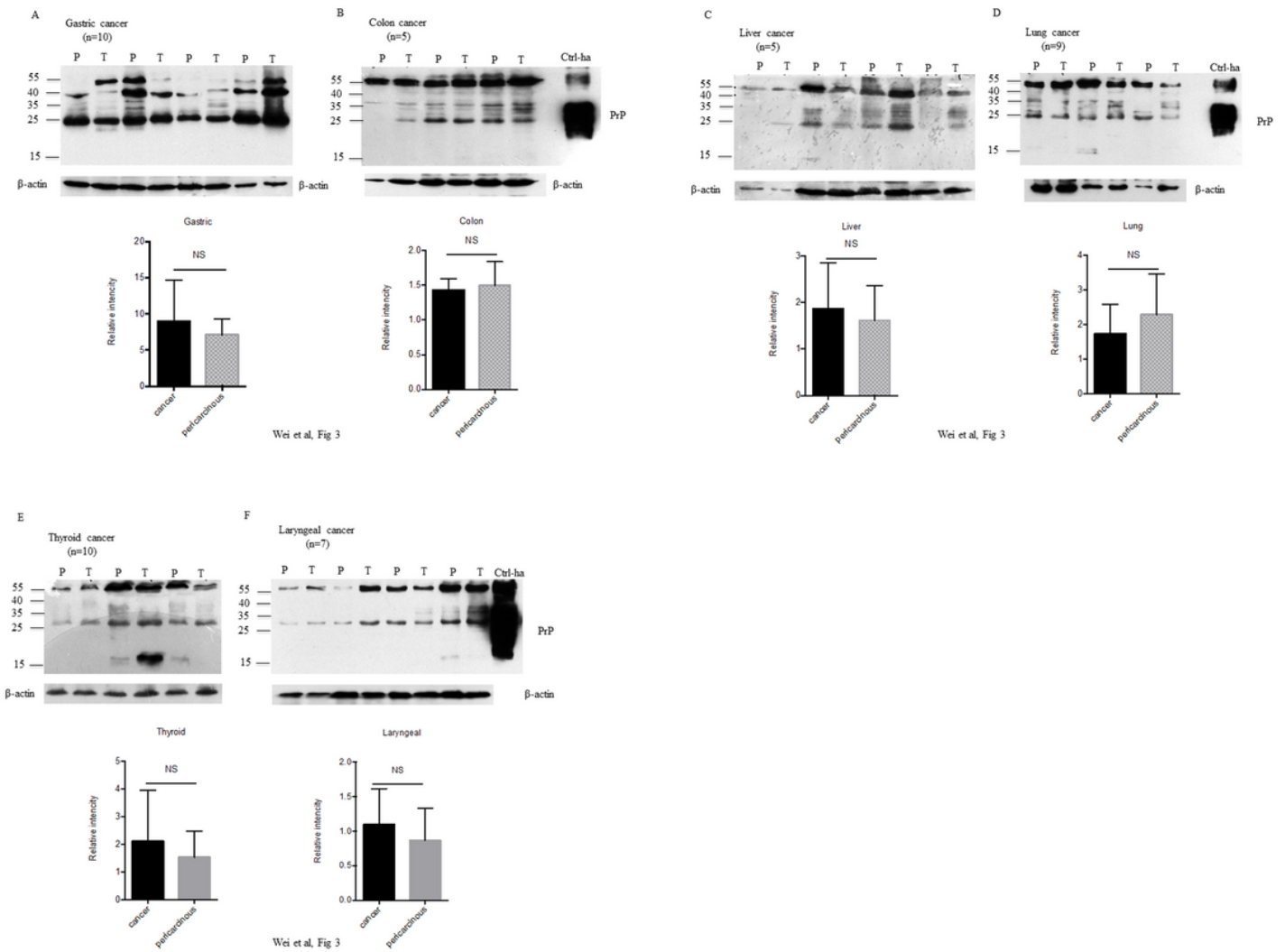
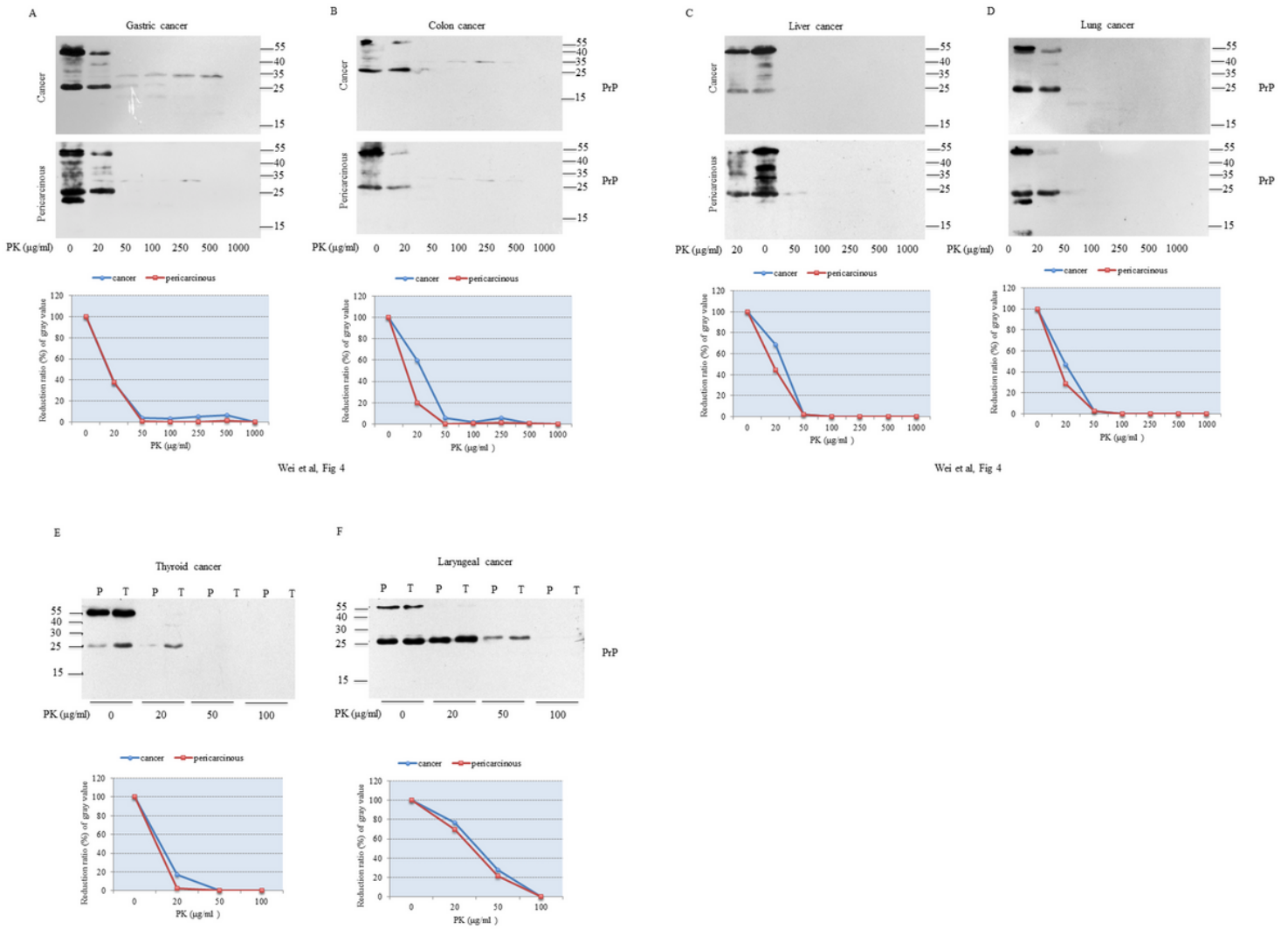


**Figure 3**

Representative Western blots of the PrPs in the homogenates of paired carcinous and pericarcinous tissues. A. Gastric cancer (n=10). B. Colon cancer (n=5). C. Liver cancer (n=5). D. Lung cancer (n=9). E. Thyroid cancer (n=10). F. Laryngeal cancer (n=7). The antibody used in Western blots was mAb 3F4. The densities of signals are determined by densitometry of all PrP signals and showed as relative intensity after normalized with the individual values of  $\beta$ -actin. Graphical data denote mean+SD and showed at the bottom of each representative graph.



Wei et al, Fig 4

Wei et al, Fig 4

## Figure 4

PK resistant activities of the PrPs in the homogenates of paired carcinous and pericarcinous tissues. The pooled homogenates of six different cancer and pericarcinous tissues were exposed to different concentrations of PK prior to SDS-PAGE. A. Gastric cancer. B. Colon cancer. C. Liver cancer. D. Lung cancer. E. Thyroid cancer. F. Laryngeal cancer. The antibody used in Western blots was mAb 3F4. The densities of signals are determined by densitometry of all PrP signals and showed as relative intensity after normalized with the individual values of  $\beta$ -actin. Graphical data of the individual tissue types are showed at the bottom of each representative graph.

## Supplementary Files

This is a list of supplementary files associated with this preprint. Click to download.

- [SuppleFig.pptx](#)